

Supplementary Materials

Variability of BVOC Emissions from Commercially Used Willow (*Salix Spp.*) Varieties

Tomas Karlsson ^{1,*}, Riikka Rinnan ² and Thomas Holst ^{1,2}

¹ Lund University, Department of Physical Geography and Ecosystem Science, Sölvegatan 12, SE-223 62 Lund, Sweden; thomas.holst@nateko.lu.se

² University of Copenhagen, Terrestrial Ecology Section, Department of Biology, Universitetsparken 15, DK-2100 Copenhagen Ø, Denmark; riikkar@bio.ku.dk

* Correspondence: tomas.karlsson@nateko.lu.se

Received: 5 February 2020; Accepted: 3 April 2020; Published: 7 April 2020

Table S1. The plot type, size (ha), previous land use, canopy height (m), soil type and content, varieties, establishment, last harvest and age (months) for the trees.

	Plot 1	Plot 2	Plot 3	Plot 4
Type	field trial	field trial	biofuel plantation	biofuel plantation
Plot size	0.07 ha	0.07 ha	5 ha	9 ha
Formerly used for	<i>Salix</i>	cereals, beets and rapes	<i>Salix</i>	<i>Salix</i>
Canopy height ¹	4.5 m	1.5 m	2.5 m	1–1.5 m
Soil type ²	loam	loam	clay loam	silty clay loam
Clay content ²	18%	24%	34%	36%
Silt content ²	34%	36%	45%	46%
Organic content ²	0%	0%	0%	0%
Varieties	Tora, Wilhelm, Ester and Inger	Tora, Wilhelm, Ester and Inger	Tora	Wilhelm
Established	2013	2017	2003	2017
Last harvest	2016	-	2017	-
Age of the trees	16 months	5 months	9 months	5 months

¹Average canopy height and age for the varieties at the last campaign at each plot.

²Taken from SGU, <http://maps-test.sgu.se:8080/TestSguMapView2/kartvisare-lerhaltskarta-sv.html> (accessed on 03-07-2019).



Figure S1. Experimental setup of leaf chamber system. To the right on the top of the tripod, the leaf chamber is attached and connected to the portable photosynthesis system (LI-6400) to the left. BVOC-sampling was done by taking a sub-sample of 200 ml/min of air leaving the leaf chamber using adsorbent tubes filled with Tenax TA and Carbograph with a small flow regulated pump.

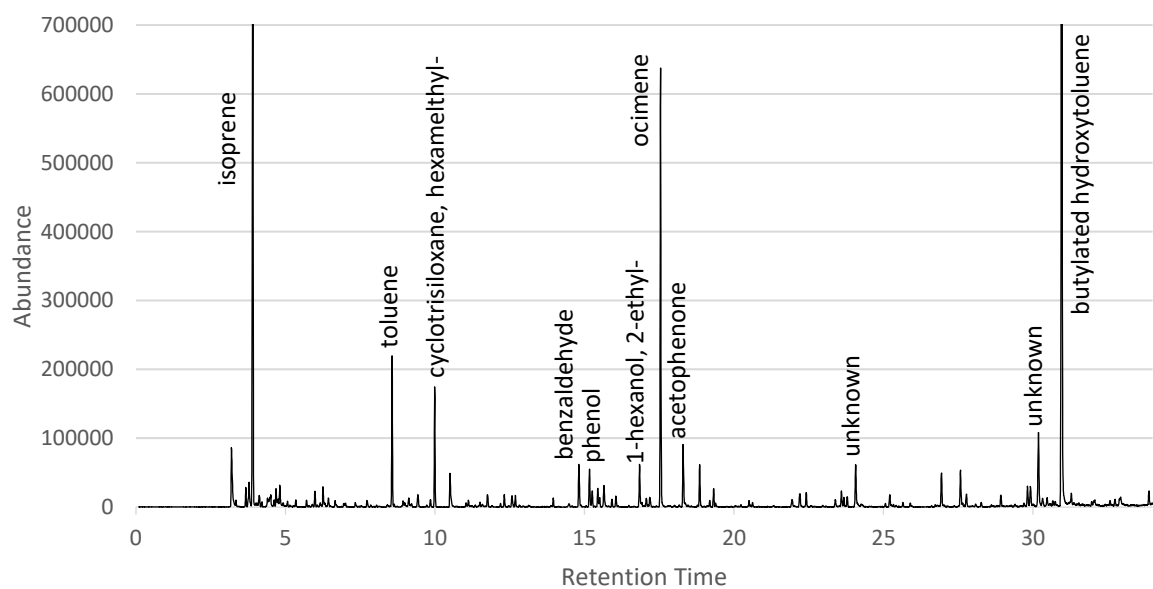


Figure S2. Total ion chromatogram sequence from a sample in GC-MS instrument where some of the most abundant peaks are identified. This measurement was taken on Inger at PAR 1500 $\mu\text{mol m}^{-2} \text{s}^{-1}$ and chamber temperature 19.5 °C.

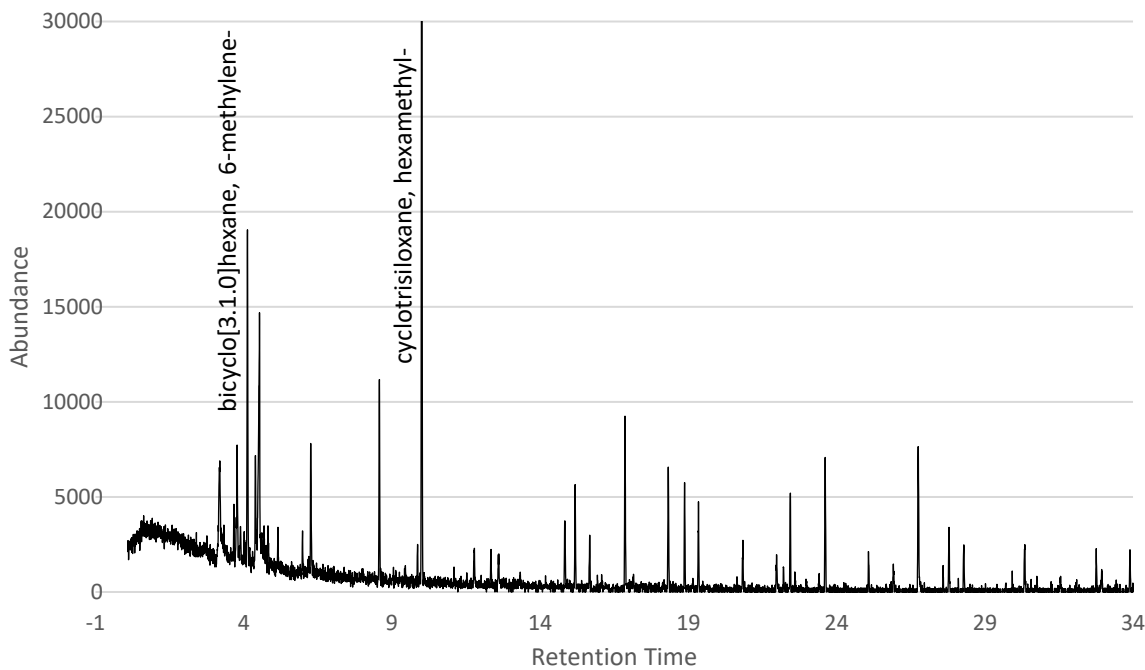
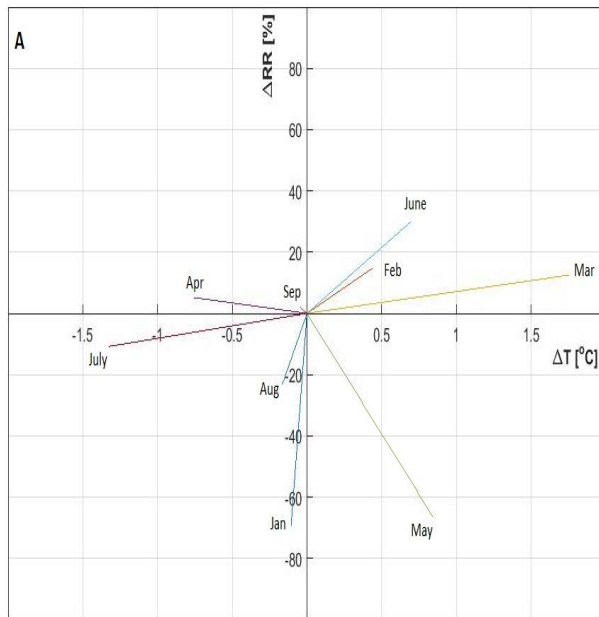


Figure S3. Total ion chromatogram sequence from a background sample in GC-MS instrument. Only bicyclo[3.1.0]hexane, 6-methylene- and cyclotrisiloxane, hexamethyl- had enough abundance to be detected in ChemStation.



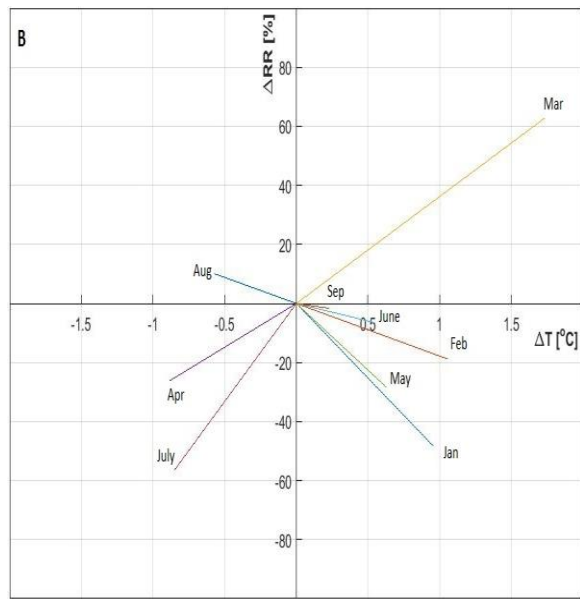


Figure S4. Thermopluiogram for plot 1 and 2 (A), and 3 and 4 (B). Values on y- and x-axis are the relative difference for precipitation, ΔRR (%), and temperature, ΔT ($^{\circ}$ C), for each month (January–September) in 2017 compared to the average monthly values between 1987–2016 (for T plot 1–4 and precipitation plot 1 and 2) and 1992–2016 (for precipitation plot 3 and 4). Data is taken from SMHI.

Table S2. Average values for ambient T ($^{\circ}$ C), T inside the leaf chamber, ambient PAR ($\mu\text{mol m}^{-2} \text{s}^{-1}$) during the measurements and growing degree days (GDDs, $^{\circ}$ C) for each day when measurements were done. No values of ambient T and PAR could be recorded on site 1 on 29 May (x) because of battery failure. No PAR was measured on 15 June (-) on site 3.

Plot 1	29 May	31 May	5 July	6 July	22 July	25 July	28 August	29 August
Ambient T ($^{\circ}$ C)	x	13.9	18.5	19.8	20.6	18.8	19.8	23.2
Chamber T ($^{\circ}$ C)	16.0	15.0	17	19.0	20.0	19.5	17.5	22.9
Ambient PAR ($\mu\text{mol m}^{-2} \text{s}^{-1}$)	x	471	1344	1474	1085	417	1019	1132
GDDs ¹ ($^{\circ}$ C)	335.6	348.3	757.9	768.9	957.1	993.9	1424.8	1437.0
Plot 2	2 June	5 June	9 July	10 July	26 July	28 July	30 August	31 August
Ambient T ($^{\circ}$ C)	19.0	18.6	20.1	21.0	21.7	20.9	19.9	16.6
Chamber T ($^{\circ}$ C)	18.0	18.2	18.3	20.0	19.3	20.0	20.9	16.8
Ambient PAR ($\mu\text{mol m}^{-2} \text{s}^{-1}$)	891	1235	1393	801	1015	1281	324	206
GDDs ¹ ($^{\circ}$ C)	380.7	409.5	792.1	805.4	1005.5	1033.5	1450.2	1465.2
Plot 3	15 June	15 July	15 July	1 August	1 August	7 September		
Ambient T ($^{\circ}$ C)	20.9	22.3	22.3	21.6	22.0	16.3		
Chamber T ($^{\circ}$ C)	20.2	20.9	21.0	20.9	21.0	14.0		
Ambient PAR ($\mu\text{mol m}^{-2} \text{s}^{-1}$)	-	1363	1350	1194	1218	801		
GDDs ¹ ($^{\circ}$ C)	386.1	708.0	708.0	896.4	896.4	1263.3		
Plot 4	13 June	28 June	28 June	12 July	13 July	14 July	2 August	5 September
Ambient T ($^{\circ}$ C)	19.3	22.6	22.6	21	21.6	23.0	20.6	15.7
Chamber T ($^{\circ}$ C)	19.2	21.3	20.7	19.5	21.1	20.9	19.8	15.0
Ambient PAR ($\mu\text{mol m}^{-2} \text{s}^{-1}$)	902	1112	1100	1061	1339	1389	919	177
GDDs ¹ ($^{\circ}$ C)	365.0	526.8	526.8	677.7	688.8	697.5	908.5	1245.3

¹GDDs was calculated as $\Sigma[(T_{\max}+T_{\min})/2 - T_{\text{base}}]$ for each starting from 1 jan 2017. $T_{\text{base}} = 5^{\circ}\text{C}$ and if $(T_{\max}+T_{\min})/2 < 0$, then $(T_{\max}+T_{\min})/2 - T_{\text{base}} = 0$.

Table S3. Values used for the fitted curves in figure 6–9. Es is STD emission rate ($\mu\text{g g}_{\text{dw}}^{-1} \text{ h}^{-1}$), C_T is correction factor for temperature described by eq. 4, α and C_{L1} are coefficient used in eq. 3 and R is Pearson's correlation coefficient for the curves. No emission of caryophyllene (-) was observed for Wilhelm.

	isoprene				ocimene			
	Tora	Wilhelm	Ester	Inger	Tora	Wilhelm	Ester	Inger
Es	20.4	95.1	41.5	98.1	9.0	13.9	0.2	8.6
C_T	0.2423	0.2423	0.239	0.2423	0.2423	0.2423	0.239	0.2423
α	0.0004	0.0004	0.002	0.0006	0.0002	0.0005	0.0002	0.0001
C_{L1}	3.91	2.73	1.23	1.15	4.49	0.47	3.73	4.37
R	0.983	0.985	0.987	0.992	0.995	0.987	0.972	0.988
	linalool				caryophyllene			
	Tora	Wilhelm	Ester	Inger	Tora	Wilhelm	Ester	Inger
Es	0.9	0.7	0.1	0.1	0.1	-	0.1	1.7
C_T	0.2423	0.2423	0.239	0.2423	0.2423	0.2423	0.239	0.2423
α	0.0009	0.0012	0.05	0.0013	0.0001	-	0.05	0.0005
C_{L1}	2.44	1.56	0.55	3.13	4.57	-	0.82	0.62
R	0.979	0.981	0.296	0.897	0.951	-	0.294	0.978

Table S4. The 20 most abundant identified BVOCs ($\mu\text{g g}_{\text{dw}}^{-1} \text{ h}^{-1}$, mean \pm standard deviation, $n = 24$ –50) for the different varieties and the first growing season trees.

T1 (plot 2)		T1 (plot 3)	
octanal	6.85 (14.40)	isoprene	5.02 (9.60)
isoprene	3.10 (4.55)	acetophenone	2.11 (4.76)
hexanal	2.32 (7.11)	ocimene	1.48 (2.12)
tridecane	1.44 (2.46)	benzaldehyde	0.73 (1.31)
heptanal	0.98 (2.77)	nonanal	0.42 (0.96)
ocimene	0.97 (1.04)	2-cyclopenten-1-one	0.29 (0.73)
1-hexanol, 2-ethyl-	0.89 (1.47)	nerolidol	0.24 (0.41)
benzaldehyde	0.83 (1.96)	linalool	0.22 (0.33)
decanal	0.80 (1.21)	octanal	0.19 (0.54)
2-heptanone	0.79 (1.56)	2,5-cyclohexadiene-1,4-dione, 2,6-bis(1,1-dimethylethyl)-	0.17 (0.29)
2-hexanone	0.73 (1.87)	phenol	0.16 (0.30)
furfural	0.67 (2.01)	o-xylene	0.14 (0.22)
nerolidol	0.59 (0.76)	p-xylene	0.13 (0.32)
tetradecane	0.56 (0.83)	2-pentanone	0.13 (0.33)
pentanoic acid, 2-ethylhexyl ester	0.55 (0.82)	furfural	0.13 (0.34)
o-xylene	0.51 (1.04)	2-cyclohexen-1-one	0.12 (0.28)
p-xylene	0.46 (0.47)	α -humulene	0.12 (0.28)
limonene	0.45 (0.71)	hexanoic acid, 2-ethyl-	0.12 (0.25)
acetic acid, butyl ester	0.45 (1.09)	cis-3-hexenyl	0.11 (0.23)
2-cyclopenten-1-one	0.44 (0.90)	2-heptanone	0.11 (0.30)
W1 (plot 2)		W1 (plot 4)	
isoprene	10.58 (18.47)	isoprene	16.01 (23.65)
acetophenone	2.37 (3.76)	hexanal	6.36 (21.95)
nonanal	1.78 (3.72)	2-pentanone	0.86 (3.94)
octanal	1.27 (2.38)	phenol	0.55 (0.83)
1-hexanol, 2-ethyl-	1.13 (1.68)	nonanal	0.38 (0.45)
tridecane	0.80 (1.61)	acetophenone	0.36 (0.51)
decanal	0.77 (1.28)	ocimene	0.35 (0.72)

benzaldehyde	0.66 (1.08)	benzaldehyde	0.31 (0.98)
pentanoic acid, 2-ethylhexyl ester	0.65 (1.21)	decanal	0.29 (0.38)
phenol	0.63 (0.80)	3-pentanone, 2-methyl-	0.27 (1.21)
phenylmaleic anhydride	0.45 (0.70)	tetradecane	0.27 (0.32)
2-heptanone	0.44 (0.85)	tridecane	0.22 (0.29)
hexanal	0.44 (1.05)	p-xylene	0.20 (0.55)
o-xylene	0.42 (0.67)	pentanoic acid, 2-ethylhexyl ester	0.20 (0.31)
tetradecane	0.39 (0.81)	nerolidol	0.16 (0.45)
furfural	0.39 (0.99)	bicyclo[3.1.0]hexane, 6-methylene-	0.10 (0.19)
undecane	0.34 (0.57)	linalool	0.10 (0.27)
ocimene	0.33 (0.48)	o-xylene	0.09 (0.17)
benzoic acid	0.32 (0.61)	pentadecane	0.08 (0.17)
2-cyclopenten-1-one	0.31 (0.60)	phenylmaleic anhydride	0.07 (0.33)
E1		I1	
isoprene	5.48 (8.36)	isoprene	6.60 (9.29)
hexanal	4.92 (6.53)	limonene	1.61 (5.55)
benzaldehyde	3.20 (4.56)	benzaldehyde	0.90 (1.13)
furfural	3.07 (3.93)	hexanal	0.83 (1.72)
octanal	3.01 (4.79)	pentane, 2-methyl-	0.73 (3.10)
acetophenone	2.46 (3.97)	furfural	0.70 (1.42)
2-cyclopenten-1-one	1.07 (1.56)	phenol	0.56 (0.74)
nonanal	0.95 (1.61)	1-hexanol, 2-ethyl-	0.47 (0.33)
2-hexanone	0.88 (1.22)	nerolidol	0.43 (0.69)
nerolidol	0.86 (1.27)	decanal	0.36 (0.33)
p-xylene	0.85 (1.96)	octanal	0.35 (0.56)
phenol	0.82 (1.20)	nonanal	0.33 (0.59)
heptanal	0.80 (1.11)	p-xylene	0.30 (0.62)
camphene	0.79 (3.96)	hexanoic acid, 2-ethyl-	0.27 (0.35)
o-xylene	0.75 (1.16)	propanoic acid, 3-ethoxy-, ethyl ester	0.25 (1.17)
1-hexanol, 2-ethyl-	0.73 (0.72)	β -pinene	0.23 (0.61)
2-heptanone	0.70 (0.99)	butane, 2-methyl-	0.23 (0.26)
2-pentanone	0.66 (0.95)	o-xylene	0.21 (0.42)
limonene	0.60 (1.58)	γ -terpinene	0.20 (0.75)
hexanoic acid, 2-ethyl-	0.57 (0.98)	α -humulene	0.18 (0.32)

© 2020 by the authors. Licensee MDPI, Basel, Switzerland. This article is



an open access article distributed under the terms and conditions of the

Creative Commons Attribution (CC BY) license

(<http://creativecommons.org/licenses/by/4.0/>).